Cell

Dissecting Timing Variability in Yeast Meiosis

Iftach Nachman,[1,2] Aviv Regev,[2,3] and Sharad Ramanathan[1,4,*]
[1]FAS Center for System Biology, Harvard University, 7 Divinity Avenue, Cambridge, MA 02138, USA
[2]Broad Institute of MIT and Harvard, 7 Cambridge Center, Cambridge, MA 02142, USA
[3]Department of Biology, Massachusetts Institute of Technology, 77 Massachusetts Avenue, Cambridge, MA 02139, USA
[4]Bell Laboratories, Alcatel-Lucent, 600 Mountain Avenue, Murray Hill, NJ 07974, USA
*Correspondence: sharad@cmt.harvard.edu
DOI 10.1016/j.cell.2007.09.044

SUMMARY

Cell-to-cell variability in the timing of cell-fate changes can be advantageous for a population of single-celled organisms growing in a fluctuating environment. We study timing variability during meiosis in *Saccharomyces cerevisiae*, initiated upon nutritional starvation. We use time-lapse fluorescence microscopy to measure the timing of meiotic events in single cells and find that the duration of meiosis is highly variable between cells. This variability is concentrated between the beginning of starvation and the onset of early meiosis genes. Cell-cycle variability and nutritional history have little effect on this timing variability. Rather, variation in the production rate of the meiotic master regulator Ime1 and its gradual increase over time govern this variability, and cell size effects are channeled through Ime1. These results tie phenotypic variability with expression dynamics of a transcriptional regulator and provide a general framework for the study of temporal developmental processes.

INTRODUCTION

In response to changing environmental conditions, cells can change their physiological state. Such changes are often mediated by a master transcription factor that is activated by environmental stimuli and in turn triggers a developmental program. The cells progress through stages of this program until they reach their final state (e.g., Figure 1A). The program often includes a commitment point, after which the cells advance irreversibly toward the final state independent of external stimuli. Cell-fate commitment is observed both in the development of multicellular organisms (Edlund and Jessell, 1999; Gilbert, 2006) and upon environmental stress in unicellular organisms (e.g., sporulation in *Saccharomyces cerevisiae* [Simchen et al., 1972], sporulation in *Bacillus subtilis* [Errington, 2003], and switching to filamentous growth in *Candida albicans* [Biswas and Morschhauser, 2005]).

Developmental irreversibility implies that mistaken decisions could be costly. An individual cell can minimize such mistakes by integrating the environmental stimuli over as long a time as possible, averaging over rapid fluctuations. This averaging delays commitment and could be lethal to a unicellular organism. In a population of such organisms, a large cell-to-cell variability in the timing of cell-fate commitment could be an alternative survival strategy (Figure 1B). The resulting phenotypic diversity could be advantageous in a fluctuating environment, as different states of the cell are better suited for different conditions. For example, in *S. cerevisiae*, while the budding cells reproduce rapidly in rich nutrients, the dormant spores can survive in extremely harsh conditions. Through variability in the timing of commitment, a deterministic developmental switch can achieve some of the advantages that have been reported for stochastic switching (Kussell and Leibler, 2005; Thattai and van Oudenaarden, 2004; Wolf et al., 2005).

Meiosis in diploid yeast cells is an irreversible developmental process triggered by nutritional deprivation, through the expression of the master regulator Ime1 (Kassir et al., 1988; Mandel et al., 1994; Simchen and Kassir, 1989). Ime1 is highly regulated at multiple levels (Figure 1D). IME1 promoter is one of the longest in yeast, containing multiple regulatory sites on which different signals converge (Granot et al., 1989; Sagee et al., 1998). The Ime1 protein activates meiotically expressed genes in several waves. One of the early targets of Ime1, the Ime2 protein, downregulates Ime1's protein levels (Guttmann-Raviv et al., 2002) and transcription (Shefer-Vaida et al., 1995), thus establishing a negative feedback loop. There is also evidence for positive feedback at the transcription level of Ime1 (Shenhar and Kassir, 2001). Additional levels of regulation of Ime1 include protein translation (Sherman et al., 1993), localization to the nucleus (Colomina et al., 1999; Colomina et al., 2003), protein activation (Bowdish et al., 1994; Rubin-Bejerano et al., 2004), and mRNA stability (Clancy et al., 2002). The developmental program controlled by Ime1 leads to meiosis and sporulation. One round of DNA replication and two rounds of nuclear division (termed *MI* and *MII*) are followed by spore

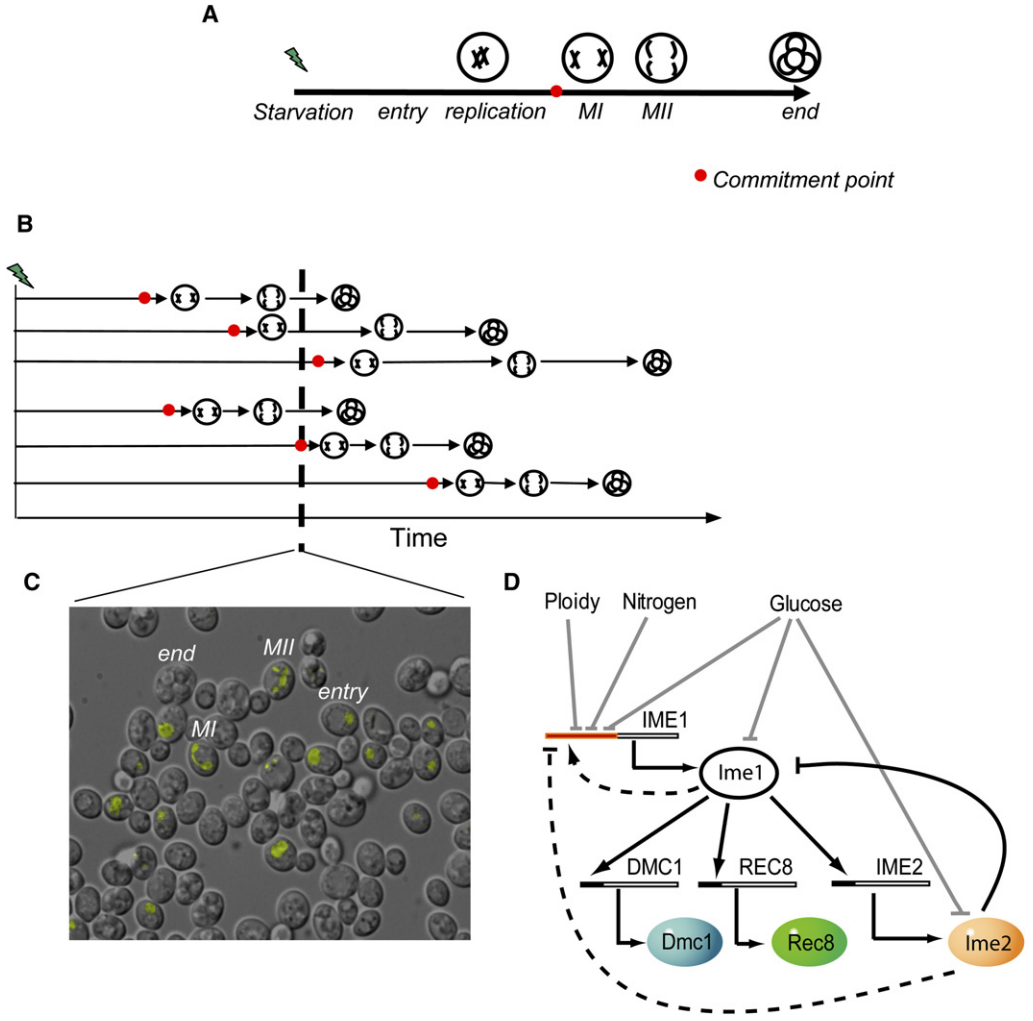

Figure 1. Timing Variability Induces Temporary Phenotypic Variability

(A) A schematic of the developmental stages during meiosis. Starvation signals (lightning bolt) activate a transcriptional cascade through a master transcription factor (TF). This cascade triggers one round of replication followed by two rounds of nuclear division (*MI* and *MII*). The red dot marks the "commitment" point, after which cells will complete the process regardless of external signals.

(B) Cells progress at different rates through different stages, resulting in phenotypic variability at a given time point. The top three cells show an even spread of the timing variability over the entire process. In the bottom three cells, this variability is concentrated before commitment. At a given time (e.g., dashed line), the population shows a diversity of intermediate states, in particular a distribution between pre- and postcommitment states.

(C) An overlay of DIC and YFP channels for cells expressing Dmc1-YFP, an early meiotic gene and a marker of meiotic chromosomes, 12 hr after a shift to sporulation conditions. The picture illustrates the large cell-to-cell variability in the developmental stage, with some cells yet to begin meiosis and others having completed sporulation.

(D) Meiosis initiation pathway. In diploids, the IME1 promoter is activated by glucose and nitrogen depletion. Once activated and localized to the nucleus, the Ime1 protein, a transcriptional master regulator, activates several initial meiosis genes, including IME2, DMC1, and REC8. Ime2 down-regulates Ime1 both at the protein and the promoter level. Dashed lines indicate regulation through unknown, possibly indirect, mechanisms.

wall biosynthesis, resulting in four haploid spores encapsulated in an ascus (Figure 1A). A commitment point to meiosis has been associated with the time of spindle pole body separation preceding *MI* (Horesh et al., 1979).

Here, we measure the cell-to-cell variability in the timing of several steps in the developmental process of meiosis in budding yeast and study the factors controlling this variability. By following several thousand cells at a time going through meiosis, we show a large cell-to-cell variability in timing of meiotic events, mostly in precommitment stages. We then analyze the sources of this timing variability, considering the effects of multiple factors such as cell size, nutritional history, cell-cycle phase, and IME1 activity. Our results reveal that cell size has an important effect on timing variability, while nutritional history and cell-cycle phase at the onset of the signal do not. In fact, early preparation for meiosis progresses in parallel to the mitotic cycle. We find that the integrated promoter activity of the

master transcription factor IME1 is a dominant factor in determining the onset time of the early meiotic program. Our results suggest that Ime1 protein accumulates gradually and thus integrates external environmental conditions as a function of time so as not to begin the downstream transcriptional program prematurely.

RESULTS

A Reporter-Based System for Single-Cell Event Timing during Meiosis

To study timing variability in sporulation, we placed diploid yeast cells with fluorescent markers in a flow chamber with multiple channels that allowed for exchange of aerated media, and we followed up to 4000 single cells at 5–10 min intervals under a fluorescent microscope for 18–45 hr as they underwent meiosis. External factors (temperature, nutrient flow) were kept constant and uniform across cells. The image sequences obtained were analyzed automatically. This setup allowed us to monitor several events during meiosis, follow protein level or promoter activity of selected genes over time, collect statistics, and correlate different features at the single-cell level.

We measured expression levels of four early meiosis genes, each tagged in a separate strain. All four genes (Ime2, Dmc1, Rec8, and Mei5) are activated by Ime1 through its interaction with Ume6 (Harbison et al., 2004; Pnueli et al., 2004; Primig et al., 2000; Rubin-Bejerano et al., 1996; Williams et al., 2002). All four proteins showed a very large cell-to-cell variability of onset times. Following onset of expression, they all showed increasing levels with time. The time courses of expression of Ime2-YFP, Dmc1-YFP, and Rec8-YFP in single cells from one experiment are shown in Figure 2. Of these four proteins, Dmc1 is the most abundant and was visible even after the end of *MII*. This enabled us to monitor both *MI* and *MII* in strains with DMC1-YFP (Figure 1C, see Movie S1 in the Supplemental Data available with this article online). To document the irreversible cell-fate commitment point in our strains, we repeated the experiment, switching back to flowing rich medium after several cells had already passed *MI*. In many cells, Dmc1 levels dropped, followed by budding and mitosis, but with no exception all recorded cells that went through *MI* completed meiosis and did not revert back to mitosis (see Movie S2 and Figure S1). The data show that commitment occurs well after Dmc1 onset, but before *MI* (within 1 hr in most of the cells).

Durations of Different Phases Are Statistically Independent; Entry into Meiosis Is the Most Variable Phase

To analyze the variability in the timing of meiosis, we divided the process into two phases: from change to sporulation medium to *MI*, with duration t_{MI}, and from *MI* to *MII* with duration t_{MII}–t_{MI}. We measured these time intervals in individual cells, obtaining a distribution for each of them. Figure 3A shows the distributions of durations of these phases in a population of DMC1-YFP cells. We analyzed the variability of these distributions using the sample variance or its square root, the standard deviation (see the Supplemental Data for discussion). The pre-*MI* phase was longer and showed higher variance (mean 12.4 hr, SD 2.4 hr, n = 386) than the post-*MI* phase (Figure 3A). Different cells completed *MI* between 7 and more than 17 hr after shift to sporulation medium. Around 45% of the cells went through to *MI* during the experiments. Thus, the time of shift to sporulation medium is an extremely poor predictor of when *MI* would occur in a given cell. In contrast, the interval from *MI* to *MII* was very short (mean time of 0.6 hr) with lower standard deviation (0.2 hr), consistent with previous studies of timing in batch cultures (Williamson et al., 1983; Padmore et al., 1991). To dissect the source of precommitment variability, we further divided the time to *MI* into a first phase, up to onset of Dmc1 expression, with duration t_{Dmc1}; and a second phase, from the onset of Dmc1 expression to *MI* with duration t_{MI}–t_{Dmc1} (Figure 3B). The onset of Dmc1 was defined as the time at which Dmc1-YFP reached a predefined threshold (shown in Figure 2B). We found that the time to onset of Dmc1 (ranging from 5 to 15 hr after shift to sporulation conditions) dominated the pre-*MI* phase (and therefore the precommitment phase), accounting for 85% of the timing variance in that phase. The phase from Dmc1 onset to *MI* was much shorter, had a lower variance (4 ± 0.9 hr), and was more normally distributed. These results were reproducible between several experiments, robust to alternative definitions of onset time (including cell-specific thresholds, see the Supplemental Data), and to using Ime2 or Rec8 instead of Dmc1 (Figure S2). Thus, the onset time of production of early targets of Ime1 is very variable and is highly correlated with the time of commitment: once the expression of early downstream targets of Ime1 begins, *MI* in most cells can be predicted to happen in 4 ± 0.9 hr.

Interestingly, we saw little or no correlation between the duration of the different phases: t_{Dmc1}, t_{MI}–t_{Dmc1}, and t_{MII}–t_{MI} (Figures 3C and 3D). Thus, each phase has little or no memory of the length of the previous one. A similar independence of timing has been recently shown between the stages of the lytic cascade of bacetriophage λ (Amir et al., 2007). Such independence implies that there cannot be a common factor (such as the level of a particular protein or the physiological state of the cell) that determines the time taken by the cell to go through all of the three phases, unless that common factor fluctuates in concentration very rapidly, resulting in the loss of any memory (Pedraza and Paulsson, 2007). We can therefore study each of these three steps independently. Since time to Dmc1 onset dominates the highly variable precommitment phase, we focused on analyzing this interval.

The variability in the onset of early Ime1 targets could be due to factors upstream of the meiotic program such as internal glucose levels, nitrogen levels, differences in cell-cycle phase, and cell size between individual cells, due to the dynamics of meiotic regulators or to any combination

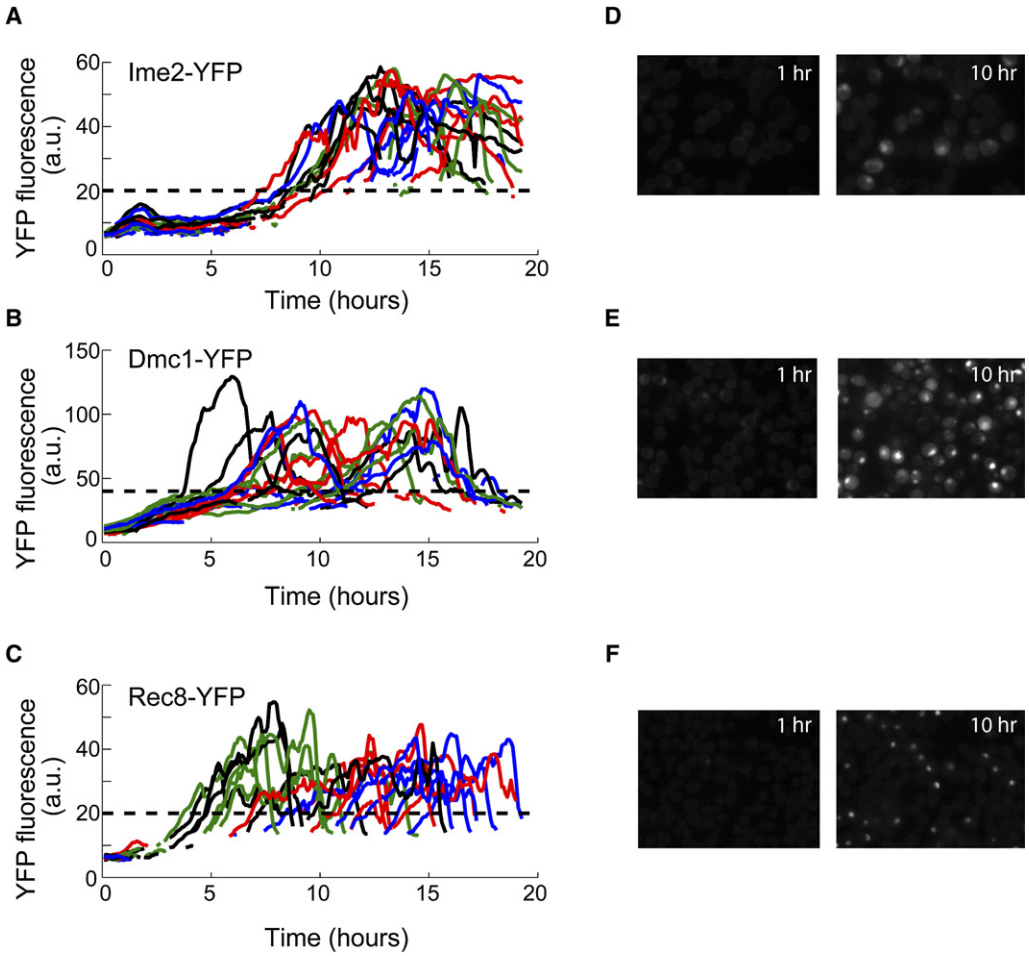

Figure 2. Time Courses of Levels of Meiotic Proteins in Single Cells Undergoing Meiosis

(A–C) Time courses of nuclear fluorescent reporter intensity for Ime1 target genes in 20 randomly sampled single cells from each of the strains Ime2-YFP (A), Dmc1-YFP (B), and Rec8-YFP (C). Each individual time course shows nuclear YFP intensity in arbitrary units plotted against the time after shift to sporulation medium. The dashed horizontal line denotes the threshold used in the definition of onset time (see text). Tracks that begin at times later than 0 correspond to cells in which no robust nuclear signal was detected at earlier times. The sharp decline in fluorescent intensity toward the end of each curve follows *MI*.

(D–F) Fluorescence images of cells 1 hr and 10 hr after the shift to sporulation conditions are shown for each of the strains corresponding to (A–C). There is a large cell-to-cell variability in the time of onset of all three genes. The duration of the experiment was 19 hr.

of the above. We studied each of these factors individually and explored the relationships between them.

Cell-Cycle Phase Has No Effect on Dmc1 Onset Time

Since our protocol does not presynchronize the cells, the variability in t_{Dmc1} could be dominated by the cell-to-cell variability in the phase of their mitotic cycle at the time of shift to sporulation conditions or by the number of mitotic cycles that the cell goes through after the shift. To test this, we repeated the experiment with a strain carrying Dmc1-YFP and a fluorescent histone (Htb2-mCherry) that allowed us to monitor nuclear mitotic events. We used the last mitotic nuclear division before initiation of meiosis in the mother cell as a landmark event for cell-cycle phase.

We found that Dmc1 expression only begins after the completion of the last mitosis. However, beyond this correlation, Dmc1 onset time (t_{Dmc1}) is independent of the duration from the shift to sporulation conditions to the last mitosis, $t_{mitosis}$. This follows from the fact that the standard deviation of the distribution of t_{Dmc1} (2.2 hr) is not larger than the standard deviation of the distribution of t_{Dmc1}-$t_{mitosis}$ (2.3 hr) (Figure 3E). Consistent results were obtained when using last budding time instead of mitosis time in the original Dmc1-YFP single color strain (data not shown). Cell-cycle phase has been shown to regulate Ime1 through the cyclin genes by controlling its localization to the nucleus (Colomina et al., 1999). The independence we find suggests that this regulation is not a limiting factor in the dynamics of meiosis initiation.

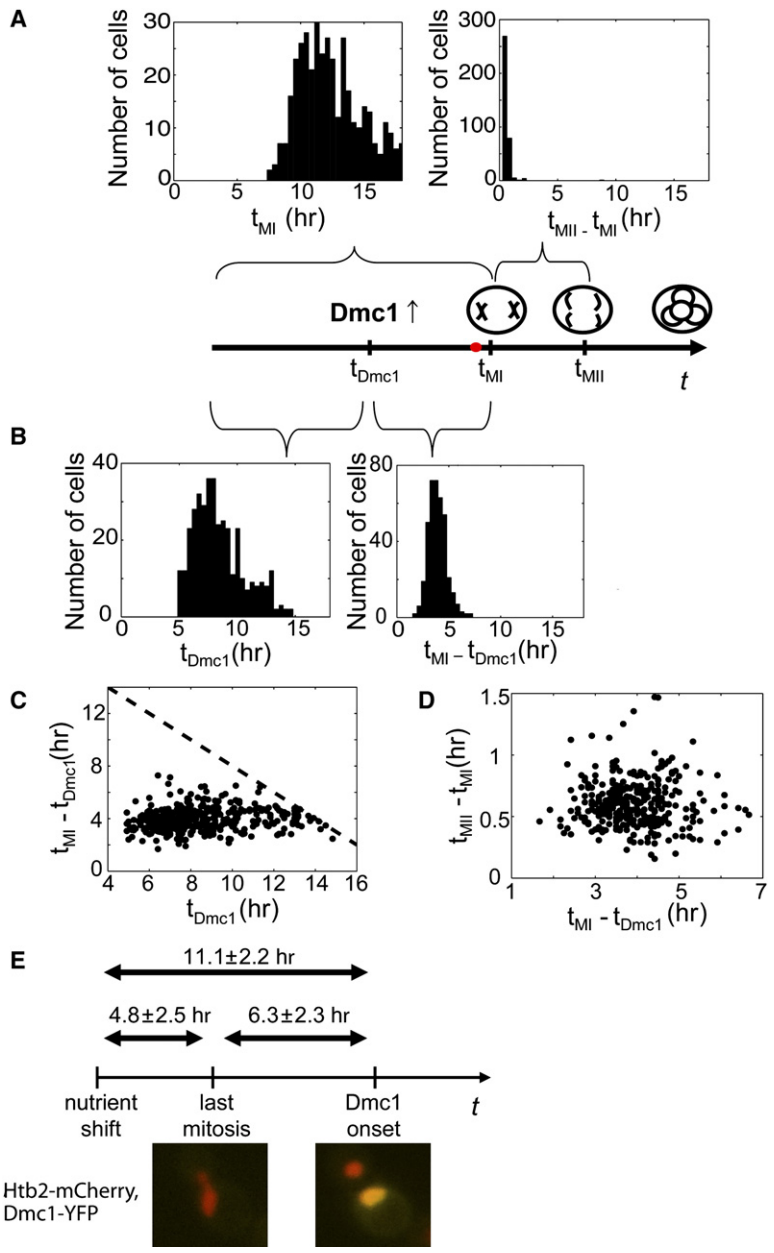

Figure 3. Distinct Phases of Meiosis Have Uncorrelated Duration, Onset Time of Early Meiosis Genes Dominates Precommitment Variability, and the Onset Time Does Not Depend on the Last Mitosis Time

(A) Timing variability of pre- and postcommitment phases. Shown are the distributions of durations in single cells of the precommitment interval (t_{MI}, from shift of nutrients to *MI*, Left panel) and the postcommitment interval (t_{MII}–t_{MI}, right panel). The precommitment interval is highly variable from cell to cell (mean 12.4 hr, SD 2.4 hr, n = 386), whereas the postcommitment interval is far less variable (mean 0.6 hr, SD 0.2 hr).

(B) Decomposition of the precommitment phase to two subphases: shown are the distributions of durations in single cells from shift of nutrients to onset of Dmc1-YFP expression (t_{Dmc1}, left panel) and from onset of Dmc1-YFP to *MI* (t_{MI}–t_{Dmc1}, right panel). The time to Dmc1 onset is far more variable (mean 8.5 hr, SD 2.2 hr) than the following subphase (mean 4.0 hr, SD 0.9 hr) and accounts for 85% of precommitment timing variance.

(C and D) Distinct phases of meiosis have uncorrelated duration. Shown are scatter plots for single cells of t_{MI}–t_{Dmc1} versus t_{Dmc1} (C) and t_{MII}–t_{MI} versus t_{MI}–t_{Dmc1} (D). The dashed line marks the end of the experiment. The durations of these phases show no correlation, indicating that knowing how long a cell spent in one phase relative to the mean gives us no information about how much time it will spend in any other phase.

(E) Dependence of Dmc1 onset time (t_{Dmc1}) on last mitosis time in mother cells in an HTB2-mCherry/HTB2, DMC1-YFP/″ strain. Shown are the mean and standard deviation for the full time interval to Dmc1 onset as well as for the subphases from nutrient shift to last mitosis and from last mitosis to Dmc1 onset. Last mitosis time is defined here as the time of the last nuclear division. Knowledge of the last mitosis time does not reduce the variance of Dmc1 onset time, as the standard deviation for the interval between the last mitosis and Dmc1 onset (2.3 hr) is not smaller than the standard deviation of the whole interval (2.2 hr). N = 108.

Ime1 Dynamics and Its Effect on Dmc1 Onset Time

To understand the sources of variability in the onset of expression of Ime1 targets, we studied the dynamics of IME1 at multiple levels. First, we estimated the levels of active Ime1 protein from the expression level of its targets. We then showed that these are comparable to measured total Ime1 protein levels (active or not). Finally, we measured the IME1 promoter activity and showed that it predicts much of the observed timing variability in the targets.

The early Ime1 targets we study have different promoter compositions, and their expression could be affected by unknown factors in addition to Ime1. We therefore estimate the temporal profile of active Ime1 protein from the measured expression time course of its downstream targets DMC1 and IME2 (Figure 4A) under the hypothesis that Ime1 is their sole regulator. A consistent estimate from both target genes would support our hypothesis. We use the following model,

$$\frac{dY}{dt} = \alpha(Ime1p) - \frac{1}{\tau_{mRNA}}Y,$$

$$\frac{dy}{dt} = \beta Y - \frac{1}{\tau_{prot}}y,$$

in which, Y and y are the mRNA and protein levels of the target gene, respectively; $\alpha(Ime1p)$ is the transcription

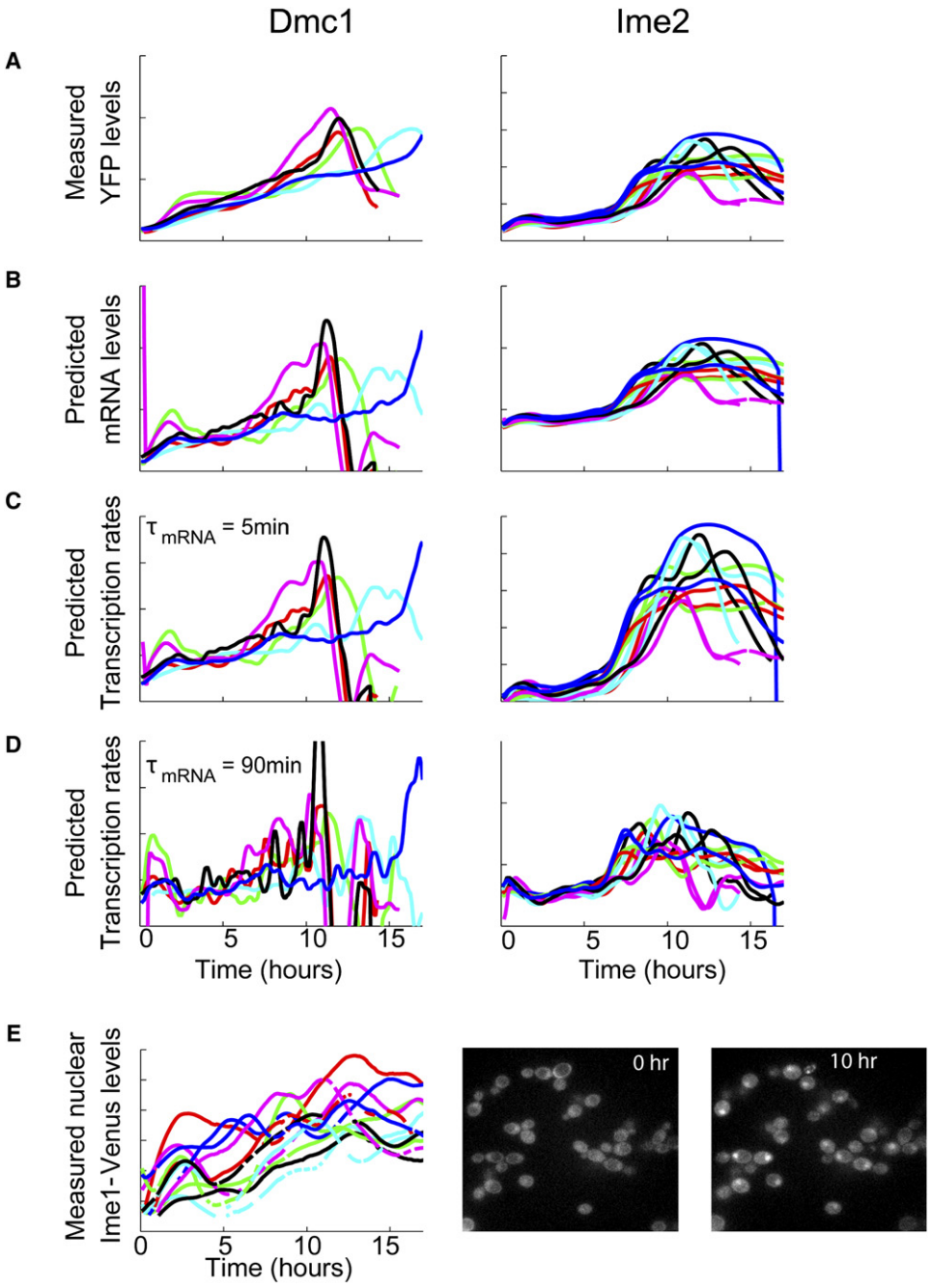

Figure 4. Measured Ime1 Nuclear Protein Levels Correspond to Active Ime1 Levels Estimated from Ime1 Targets

(A–D) A model predicting the time behavior of active Ime1 levels: (A) time courses of YFP intensity levels in several sample cells of Dmc1-YFP (left) or Ime2-YFP (right) strains from the experiment shown in Figure 2. The curves drop sharply after the time corresponding to *MI*. (B) Computed mRNA levels of Dmc1 or Ime2 in the corresponding cells. The computation was done using protein half-lives of 92 min (Dmc1) and 5 min (Ime2). (C and D) mRNA transcription rates computed for the same cells from the predicted mRNA levels, using an mRNA half-life of 5 min (C) or 90 min (D). The active Ime1 protein levels are expected to have a similar time profile to the transcription rates.

(E) Time courses of nuclear Venus intensities in several sample cells of an Ime1-Venus strain. The qualitative behavior, in particular a gradual increase of Ime1 over several hours, corresponds to that predicted by the model for active Ime1 levels. The duration of the experiment was 24 hr.

rate of Y as a function of the active protein concentration of Ime1; τ_{mRNA} and τ_{prot} are the half-lives of the target mRNA and protein, respectively; and β is the translation rate from a single mRNA molecule of Y. Once the target protein half-life is known, we can estimate the time profile of the scaled target mRNA levels, βY, from the measured

protein profiles, *y*, and their derivatives. For Dmc1, we estimated the protein half-life τ_{prot} to be around 90 min (see the Experimental Procedures), and for Ime2, τ_{prot} has been previously estimated to be 5 min (Guttmann-Raviv et al., 2002) (Figure 4B). As the mRNA half-lives τ_{mRNA} for these genes are not known, we obtain bounds on the shape of the scaled transcription rates $\beta\alpha(Ime1p)$ (Figures 4C and 4D) by using two extreme values (5 min and 90 min), which are based on the distribution of known mRNA half-lives measured by Wang et al. (2002). All estimates lead to $\alpha(Ime1p)$ with similar features for both targets: a short initial peak followed by a gradual increase over several hours. Assuming $\alpha(Ime1p)$ is a monotonic function of the active protein levels of Ime1, it can serve as a qualitative approximation for the time behavior of these levels. Even though the qualitative behaviors of the expression of Ime2 and Dmc1 are different (Figure 2), they both result in similar predicted profiles of active Ime1 protein (Figure 4C). This suggests that the level of active Ime1 is the dominant factor determining the temporal behavior of these genes.

We compared these derived profiles to measured levels of total nuclear Ime1. We were able to detect Ime1 tagged with Venus (Nagai et al., 2002) using a sensitive camera despite its low abundance and short lifetime (Colomina et al., 2003). We found that total nuclear Ime1 protein levels show similar time profiles to those derived by our model for active Ime1 levels: an initial peak followed by decline to baseline levels, followed by gradual accumulation in the nucleus that lasts around 5 hr (Figure 4E, Movie S3). Although we could not measure Ime1 protein and its targets in the same strain, this qualitative agreement suggests that total Ime1 nuclear protein levels would be highly predictive of the behavior of its target genes and in particular their onset time.

Multiple levels of IME1 regulation can contribute to the variation in active Ime1 protein and consequently in its targets—from IME1 transcription to posttranslational modifications. We next monitored IME1 promoter activity in an ime1::NLS-mCherry/IME1 strain. mCherry folds within 40 min and does not degrade significantly. Therefore, total mCherry levels reflect the cumulative IME1 promoter activity, while mCherry time derivative reflects the instantaneous activity of that promoter. By incorporating this reporter in a Dmc1-YFP homozygous strain, we could also check the effect of IME1 promoter activity on t_{Dmc1}. In this strain, the distribution of Dmc1 onset times was slowed down by a factor of 1.3–1.5 but otherwise maintained its shape compared to a strain with two copies of IME1, thus still allowing us to faithfully study the dependence between IME1 and its target (Figure S4).

Within 2 hr of shift to sporulation medium, the promoter of IME1 is activated in all the cells, and its activity does not increase with time, as seen by the nonincreasing mCherry slopes in Figure 5A. Thus, there is very little variability in the timing of initiation of IME1 promoter activity. The immediate and full onset of IME1 promoter activity in all the cells upon nutrient deprivation is in sharp contrast to the variation in onset of Flo11, the master regulator in the switch to pseudohyphal growth (Halme et al., 2004). Consistent with our result on independence of t_{Dmc1} on mitotic phase, the onset time and the slope of mCherry are independent of the mitotic state of the cells (Figure S5).

We measured the dependence of t_{Dmc1} on the IME1 promoter activity. We found that the instantaneous promoter activity of IME1 showed maximum anticorrelation with t_{Dmc1} at 8 hr after the shift of cells to sporulation medium. Hence, cells with a higher IME1 production rate at that time tended to start Dmc1 expression earlier (Figures 5B and 5D, blue curve). Total mCherry levels showed strong anticorrelation with t_{Dmc1}. This anticorrelation increased with time (Figures 5C and 5D). Thus, cells with a higher cumulative production from the IME1 promoter start Dmc1 expression earlier.

Two lines of evidence support the predominant role of IME1 in determining the timing variability of its targets' onset. First, cumulative mRNA production of IME1 is predictive of t_{Dmc1}, despite the several levels of regulation separating it from the production of Dmc1 protein. Furthermore, nuclear Ime1 levels follow the behavior of active Ime1 levels derived from observed target protein time profiles, suggesting that Ime1 is the dominant factor in the dynamics of its targets. Interestingly, we see a gradual increase in Ime1 protein levels, despite the short lifetime of Ime1p (Colomina et al., 2003 and Figure S3) and the constant production rates observed at the promoter level. This suggests that one of the intermediate levels of regulation (e.g., Ime1 mRNA or protein stability) is gradually modulated in time.

Effect of Nutrient Signaling and Cell Size on Ime1 Dynamics and Dmc1 Onset Time

We next studied the effects of global parameters and factors upstream of the promoter of IME1 on DMC1 onset time. Through quantitative analysis, we measured how much of these effects are channeled through IME1.

First we studied the effects of glucose and nitrogen starvation on t_{Dmc1} variation. These signals affect entry into meiosis through the Ime1 promoter (Granot et al., 1989; Sagee et al., 1998) as well as through other channels (Vidan and Mitchell, 1997; Xiao and Mitchell, 2000). If any of them were a major independent source of timing variability, activating that signal ahead of the others should reduce the variability. To test this hypothesis, we pregrew the cells in media lacking either glucose or nitrogen (Experimental Procedures). In both cases, the variance of t_{Dmc1} was not reduced (Figures 6A and 6B, also see the Supplemental Data). We monitored glucose signaling by measuring the delocalization of Bcy1 from the nucleus (Griffioen et al., 2000) in BCY1-YFP cells grown in the flow chamber in rich medium and then exposed to sporulation conditions. All the cells showed Bcy1 export from the nucleus within the first 3 hr after shift to sporulation medium (Movie S4) with little variation, and the timing of Bcy1 export was not predictive of t_{Dmc1}. Thus, glucose or nitrogen sensing individually do not contribute

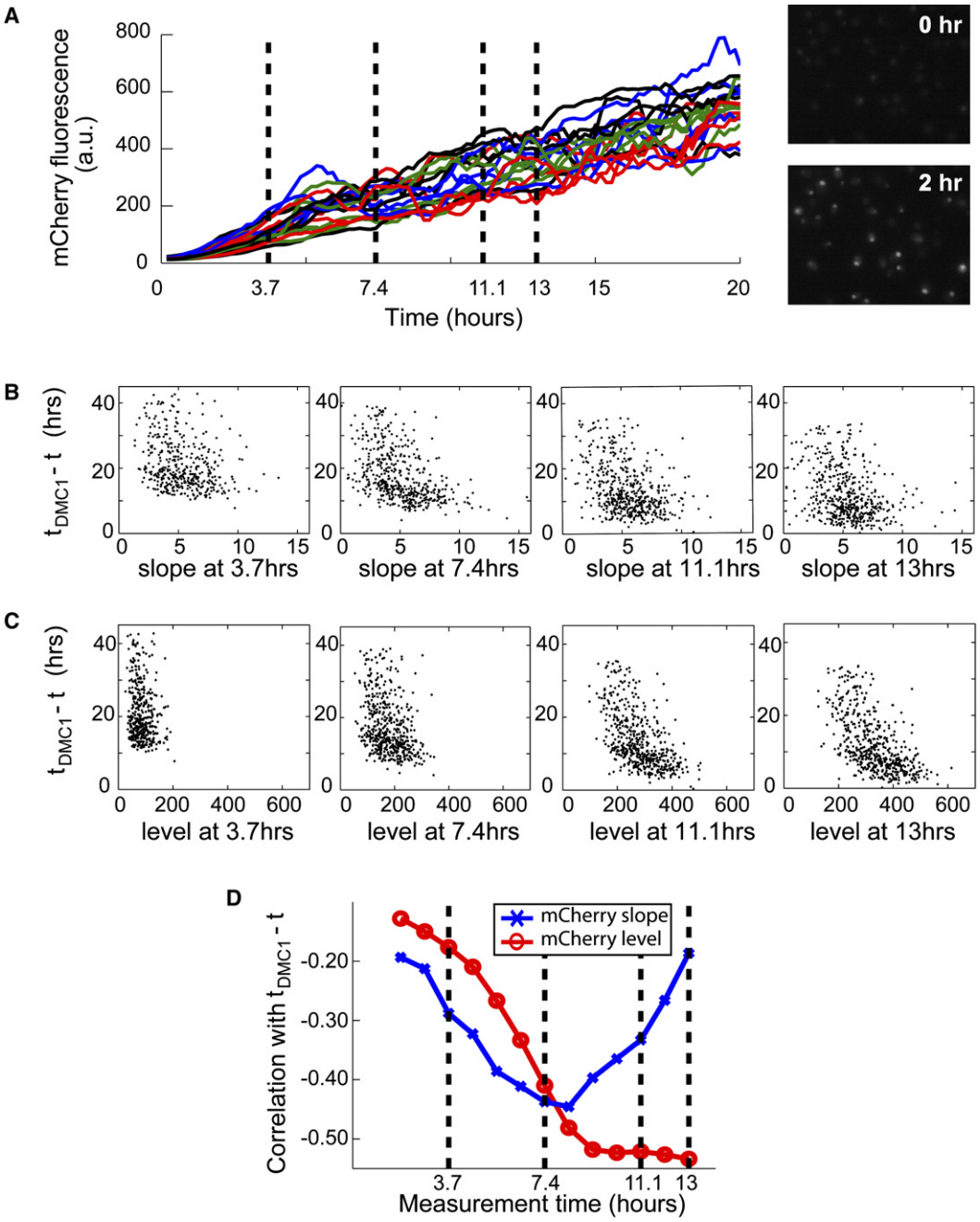

Figure 5. pIME1 Cumulative Activity Is Predictive of Dmc1 Onset Time

(A) IME1 promoter activity. Shown is promoter activity as reflected by the mCherry signal in a pIME1-NLS-mCherry/IME1, DMC1-YFP/″ strain in 20 randomly sampled single cells as a function of time during the first 20 hr after shift to sporulation medium. Promoter activity increases in all cells, with no delay from shift of nutrients. The slope and hence the rate of production of mCherry does not increase with time. The four time points indicated correspond to the plots in (B) and (C). The fluorescence images show cells at the time of and 2 hr after the shift to sporulation conditions. The duration of the experiment was 46 hr.

(B) Scatter plots of mCherry production rates (x axis, measured by local mCherry slopes) in ~500 single cells at $t = 3.7$ hr, 7.4 hr, 11.1 hr, and 13 hr after shift to sporulation medium versus remaining time to Dmc1 onset, $t_{Dmc1} - t$ (y axis). Note that Dmc1 onset only begins around 13 hr in this experiment (see also Figure S4).

(C) Scatter plots of mCherry levels (x axis) at the same time points as in (B) versus remaining time to Dmc1 onset, $t_{Dmc1} - t$ (y axis).

(D) Correlation coefficients of mCherry slopes and $t_{Dmc1} - t$ (blue x marks) and of mCherry levels and $t_{Dmc1} - t$ (red circles) shown as a function of the measurement time, t. Production rates of IME1 at intermediate times (7–11 hr) affect Dmc1 onset times 8 hr into the future (as seen by the negative correlation). However, at later times (12–14 hr), that correlation is lost. Cumulative production of mCherry, on the other hand, shows a negative correlation with $t_{Dmc1} - t$, which only increases with time.

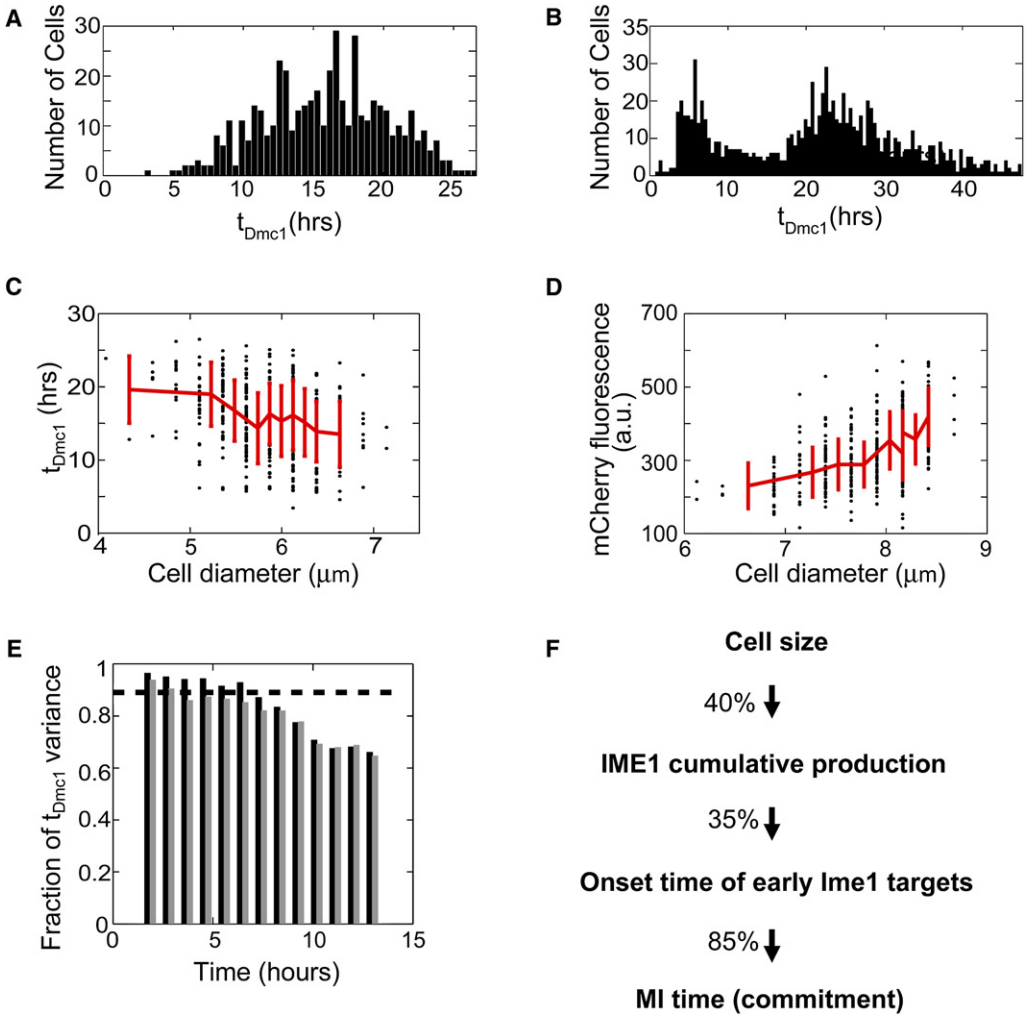

Figure 6. Contribution of Internal and External Factors to Prediction of t_{Dmc1}

(A and B) Dmc1-YFP onset time distribution for cells pregrown in YPA (no glucose) for 12 hr (A) or SLAD (low nitrogen) for 12 hr (B). Both pretreatments show no reduction in timing variance compared to Figure 3B (YPA, mean 15.4 hr, SD 4.8 hr, n = 495; SLAD, mean 21 hr, SD 11 hr, n = 939). The durations of the experiments were 27 and 48 hr, respectively.

(C) Onset time as a function of cell diameter shows a negative correlation. The red lines denote medians and standard deviations in different bins along the x axis.

(D) IME1 cumulative promoter activity (measured by pIME1-NLS-mCherry levels) at 13 hr after shift to sporulation medium versus cell diameter shows a positive correlation.

(E) The variance of t_{Dmc1} given size alone, cumulative IME1 promoter activity alone, or both. The variances given different factors were computed using the maximum likelihood estimator (see the Supplemental Data) and plotted as a fraction of the variance in the unconditional model P(t_{Dmc1}). All figures were computed on Dmc1-YFP/″, ime1::NLS-mCherry/IME1 cells in the experiment shown in Figure 5. Dashed line shows variance given size only (i.e., variance of $P[t_{Dmc1} \mid \text{cell size}]$). At each time bin (x axis), the black bar shows the variance given mCherry level alone (i.e., variance of $P[t_{Dmc1} \mid mCherry(t)]$). The gray bar shows the variance given both mCherry level and cell size (i.e., variance of $P[t_{Dmc1} \mid cell\ size, mCherry(t)]$). The difference between the black and gray bars decreases with time, showing that the effect of size on onset time is channeled through IME1.

(F) The dominant effects leading to *MI* time. The percentage of the variance in each factor that is accounted for by the previous (upstream) one is shown (e.g., 40% of the variance in IME1 cumulative production is accounted for by cell size).

significantly to variability in t_{Dmc1}. As in earlier experiments (Figure 3C), there was no correlation between the duration of the three phases for cells prestarved for glucose or nitrogen (Figure S6, compare with Figure 3C).

We then measured the effects of cell size on the variability of t_{Dmc1}. Cell size was previously shown to affect sporulation efficiency (Day et al., 2004). We found a clear negative correlation between t_{Dmc1} and cell diameter, for a cell population that started the experiment at stationary phase in which none of the cells budded before sporulating (Figure 6C). This confirms that larger cells tend to start meiosis earlier. Furthermore, cells that were smaller at

the start of the experiment grow for a longer period but stop growth at a smaller final size than cells that were larger at the beginning. This effect, as well as the negative correlation between size and t_{Dmc1}, is more pronounced in experiments in which cells undergo mitosis a few times after shift to sporulation conditions (Figure S7). We find that the long time tail of the distribution in Figure 3B is dominated by small cells. Overall, in different experiments, cell size explains between 11% and 30% of the variance in Dmc1 onset time, consistent with the results of Day et al. (2004) from experiments in batch culture. Additionally, we found no significant correlation between size and subsequent time intervals (data not shown). Thus, size contributes to cell-to-cell variability by affecting time to onset of early meiosis genes.

Cell size correlates strongly with cumulative IME1 promoter activity at later times (measured by pIME1-NLS-mCherry levels, Figure 6D), accounting for up to 40% of the cell-to-cell variance in cumulative IME1 production. How well do Ime1 levels predict Dmc1 onset time, and how much of it is already accounted for by cell size? To address this, we examined the fraction of Dmc1 onset time variance explained by integrated pIME1 activity alone, by cell size alone, or by both (Figure 6E and the Supplemental Data). We find that the ability to predict t_{Dmc1} using integrated pIME1 activity alone at a given point in time improves with time, explaining up to 35% of the variance in t_{Dmc1}. Once the integrated pIME1 activity has been accounted for, the residual variance explained by cell size decreases with time. Thus, size adds little additional information about t_{Dmc1} over that given by pIME1. This suggests that most of the effects of size on Dmc1 onset time are channeled through IME1 promoter activity.

We quantified different factors that finally lead to *MI* and commitment to meiosis in terms of how much variance each of them explains in the next step. For example, we showed that knowledge of Dmc1 onset time reduces the standard deviation of the time to *MI* from 2.4 to 0.9 hr. In other words, Dmc1 onset time explained 85% of the variance in the time to *MI*. We can similarly summarize our results in an "influence diagram" of the dominant factors leading to the time of commitment (Figure 6F): commitment timing and its variance are dominated by the onset time of early meiosis genes. Up to 35% of the variance in this onset time can be explained by cumulative IME1 production rates. The most dominant extrinsic factor we found is cell size, whose effect is largely mediated through the IME1 promoter activity.

DISCUSSION

To decide on and make any developmental change, a cell needs to measure, integrate, and accurately process several signals in its environment. Different cells in a population can decide and march toward commitment to this change at different rates. At least in multicellular organisms, the decision has to be coordinated with the mitotic state of the cell as well as with the decision of nearby cells (Gilbert, 2006).

The following questions can be asked of any developmental process: (1) how are developmental events along such a process timed in individual cells, and how is the variance in the timing distributed along the process? (2) What are the contributions of signal integration and the dynamics of master regulators to this timing? (3) How is the timing variability regulated and coordinated with mitosis?

Here, we answered these questions in the context of yeast meiosis as an example of a developmental process in a unicellular eukaryote. By combining time series measurements on a large number of cells with statistical methods, we were able to measure the timing of different events and draw both quantitative and qualitative statements on the flow of causal effects in the process. This methodology is applicable to a wide variety of cellular processes.

Timing and Variance of the Different Phases of Meiosis

We verified that in each cell the timing of commitment was close to the time of *MI*. We showed that meiosis could be broken into distinct phases, each of whose duration is independent of the others. The longest and most variable phase is the interval between the beginning of the starvation signal and the onset of Ime2, Dmc1, Mei5, or Rec8, all early meiosis genes. This phase occurs before the point of commitment (MI) and before the onset of the transcriptional response downstream of the master transcription factor Ime1. Concentrating most of the precommitment delay and variance prior to the onset of the first transcriptional wave allows some fraction of the population an easy re-entry into mitosis upon a return of nutrients.

The Role of the Dynamics of the Master Regulator Ime1 in Timing Delay and Variability

The complex promoter of IME1 enables the combinatorial processing of the levels of oxygen, nitrogen, and glucose to make sure that all the conditions for starting the program are met. We find that the IME1 promoter turns on within 2 hr of nutrient starvation in all the cells, after which point its activity remains constant at least until the onset of the transcription of early targets. From our prestarvation experiments, we concluded that glucose and nitrogen signaling alone cannot play a role in the timing of the first phase, and neither can the integration of these signals at the IME1 promoter.

We find that Ime1 protein levels in the nucleus increase gradually over time. This slow and gradual accumulation could allow the cell to integrate the signals over time, thus ensuring that nutrients are lacking in the environment for an extended period before starting the downstream transcriptional cascade. Moreover, variable accumulation rates lead to a gradually built up variance in Ime1 levels between cells, contributing to the variance in onset time of downstream targets.

Our observations that cell size effect on timing is channeled through IME1 promoter activity, and that glucose prestarvation, despite affecting meiosis through additional pathways that bypass this promoter (Honigberg and Purnapatre, 2003), has little effect on timing variance, point to IME1 as the dominant channel between external conditions and the timing of meiosis.

Coordination with the Cell Cycle: Advancing Mitosis and Meiosis in Parallel

Our experiments show that the timing of Dmc1 onset is independent of the time of the last mitosis. The position in the cell cycle of a particular cell has no predictive power on how long the onset of Dmc1 expression in that cell might take. In fact, IME1 promoter activity begins in full even in cells that are still undergoing mitosis. We also see cases of cells that bud after Ime1-Venus protein has already accumulated in their nuclei (see Movie S3). Thus, the cell can begin preparations for the meiotic program even while it is still in the mitotic cycle, advancing in these two programs in parallel for several hours. In the context of a fluctuating environment, it can be advantageous to start preparing for meiosis even while the cell is in the mitotic cycle, for as long as mechanistically possible. While on one hand the cell will not waste time returning to growth if needed, it also starts integration of the starvation signals (by accumulation of Ime1) right upon encountering them. This might be important to assure the cell still has enough internal resources to complete the complex meiotic program upon decision to commit.

Timing Variability versus Synchronization

Large cell-to-cell variability in the timing of commitment can be advantageous for a population of isogenic single cells facing a fluctuating environment. Different cells wait different periods of time before beginning the transcriptional program of hundreds of genes, many expressed well before the commitment point. The fact that oak strains, which face very different environmental conditions from vineyard strains, typically enter meiosis faster (Gerke et al., 2006) supports the connection between evolution of timing in this process and the environment statistics. The bacterium *Bacillus subtilis*, which also sporulates upon starvation, was shown to delay its commitment to sporulation by cannibalizing nonsporulating brethren, thus extending the nutrient supply and prolonging the time to decision (Gonzalez-Pastor et al., 2003). A study similar to ours on the cell-to-cell timing variability in *B. subtilis* sporulation will help better understand the commonality and differences in the strategies used by microorganisms to deal with uncertain environmental conditions.

The sets of biological constraints and evolutionary pressures on timing in multicellular organisms are very different and depend on the particular temporal process. For example, in the mitochondrial pathway of apoptosis in vertebrates we see similar features of delay and variability prior to commitment: though mitochondrial permeabilization and release of cytochrome *c* can occur anytime between 4 and 20 hr following the apoptotic signal, full activation of caspase genes (associated with commitment to apoptosis) occurs within 10 min later, and subsequent stages are shorter and less variable (Goldstein et al., 2000; Green, 2005). On the other hand, in cellular differentiation along development, one might expect developmental decisions to be tightly coordinated between cells as well as with the position of the cell in the cell cycle. Our work raises the interesting questions of how timing and timing variability are controlled in embryos, how cells therein can integrate the signal over sufficient periods of time to allow for accurate measurements while simultaneously coordinating their state with those of their neighbors during development, and how this timing is dependent on mitosis.

EXPERIMENTAL PROCEDURES

Yeast Strains and Growth Conditions

All experiments were performed on diploid cells in the SK1 strain background (Kane and Roth, 1974). Strains were constructed using standard molecular biology techniques. The strains used in this study are summarized in Table S1. In all experiments, cells were grown overnight to saturation in YPD, then diluted 1:12 into fresh YPD. After the culture was incubated at 30°C for 5–6 hr, the cells were harvested and washed twice with and resuspended in SPM + Leu (0.3% KAc, 0.02% raffinose, 100 μg/ml leucine). They were then immediately transferred to the flow chamber. The cells were never synchronized or sorted by size. About 40% of the cells completed meiosis in the flow chamber within 18 hr (Figure S8). A large fraction of the cells often underwent one to two mitotic divisions during measurements before entering meiosis. We could reduce or eliminate the mitotic cycles by growing the cells in YPD well past the diauxic shift before transferring them to sporulation medium. The statistics and correlations of timing were independent of the number of mitotic cycles cells completed in the chamber. For experiments involving prestarvation of cells for glucose or nitrogen, an overnight culture in YPD was reinoculated for 12 hr in YPA (1% KAc) or SLAD (Gimeno et al., 1992) before a shift to sporulation medium.

Flow Chamber and Attachment of Yeast Cells

The cells were placed in a flow chamber (FCS2, Bioptechs) in which the temperature was held at 28°C. They were immobilized on the coverslip using concavalin A (Sigma). Aerated SPM + Leu medium was passed over the cells at a flow rate of 10 ml/hr, corresponding to a change of the entire volume every 30 s.

Automated Time-Lapse Microscopy

The cells in the flow chamber were observed using a Zeiss 200 M fluorescent microscope with a Hamamatsu Orca-II-ER camera, a Prior ProScan II motorized stage, and a Zeiss 100×/1.45 NA Plan-FLUAR objective, all controlled by MetaMorph. Emission from YFP was visualized at 535 nm (38 nm bandwidth) upon excitation at 500 nm (20 nm bandwidth). Emission of mCherry was visualized at 650 nm (75 nm bandwidth) upon excitation at 565 nm (55 nm bandwidth). Imaging of Ime1-Venus was done using a Hamamatsu ImageEM camera, with 500 ms exposures and the same filter settings as for YFP.

Each stage position covered 30–100 cells, and up to 50 stage positions were monitored during the course of an experiment. Images were obtained from each position at fixed intervals (5–10 min). A typical experiment thus followed 1000–1500 cells over a 18–48 hr period. When strains were compared (e.g., Figures 2 and 5C), they were all pregrown in parallel and then placed simultaneously in different channels of the flow cell in a single experiment, allowing us to eliminate errors due to day-to-day variability in handling.

Data Analysis

All image processing and data analysis was done using custom-written software in MATLAB (Version 7). DIC images were used to detect single cells. Cells were then mapped between time points. Nucleic signals were detected in fluorescent images using local adaptive thresholding, and those signals were then mapped to cells. Signal density was computed as total intensity divided by number of pixels. Meiosis events were tagged automatically using a combination of features such as signal density, number of separate nucleic signals, and distance between those signals. Accuracy of event tagging was verified by hand annotation on a sample of at least 100 cells. Mitosis events were tagged manually.

The half-life of Dmc1 was estimated from Dmc1-YFP time series of 224 cells after switching back to rich medium in a return to growth experiment. The switch resulted in a drop in Dmc1-YFP levels. The time from maximal signal to half its value was taken as the half-life, resulting in an estimate of 92 ± 30 min.

Supplemental Data

Supplemental Data include supplemental text, seven figures, one table, four movies, and Supplemental References and can be found with this article online at http://www.cell.com/cgi/content/full/131/3/544/DC1/.

ACKNOWLEDGMENTS

We thank N. Kleckner, Y. Kassir, B. Stern, D. Thompson, A. Schier, G. Lahav, A. Murray, N. Barkai, R. Losick, and three reviewers for comments; the Kleckner and Amon labs for strains; K. Thorn for plasmids; and Merck Postdoctoral Fellowship (I.N.), a Burroughs Wellcome Fund CASI (A.R.), Human Frontiers Science Program Grant (S.R.), the Keck Futures Initiative Program Grant (S.R.), and National Institute of General Medical Sciences Center grant P50 GM068763 for support.

Received: February 28, 2007
Revised: July 18, 2007
Accepted: September 21, 2007
Published: November 1, 2007

REFERENCES

Amir, A., Kobiler, O., Rokney, A., Oppenheim, A.B., and Stavans, J. (2007). Noise in timing and precision of gene activities in a genetic cascade. Mol. Syst. Biol. *3*, 71. Published online February 13, 2007. 10.1038/msb4100113.

Biswas, K., and Morschhauser, J. (2005). The Mep2p ammonium permease controls nitrogen starvation-induced filamentous growth in Candida albicans. Mol. Microbiol. *56*, 649–669.

Bowdish, K.S., Yuan, H.E., and Mitchell, A.P. (1994). Analysis of RIM11, a yeast protein kinase that phosphorylates the meiotic activator IME1. Mol. Cell. Biol. *14*, 7909–7919.

Clancy, M.J., Shambaugh, M.E., Timpte, C.S., and Bokar, J.A. (2002). Induction of sporulation in Saccharomyces cerevisiae leads to the formation of N6-methyladenosine in mRNA: a potential mechanism for the activity of the IME4 gene. Nucleic Acids Res. *30*, 4509–4518.

Colomina, N., Gari, E., Gallego, C., Herrero, E., and Aldea, M. (1999). G1 cyclins block the Ime1 pathway to make mitosis and meiosis incompatible in budding yeast. EMBO J. *18*, 320–329.

Colomina, N., Liu, Y., Aldea, M., and Gari, E. (2003). TOR regulates the subcellular localization of Ime1, a transcriptional activator of meiotic development in budding yeast. Mol. Cell. Biol. *23*, 7415–7424.

Day, A., Markwardt, J., Delaguila, R., Zhang, J., Purnapatre, K., Honigberg, S.M., and Schneider, B.L. (2004). Cell size and Cln-Cdc28 complexes mediate entry into meiosis by modulating cell growth. Cell Cycle *3*, 1433–1439.

Edlund, T., and Jessell, T.M. (1999). Progression from extrinsic to intrinsic signaling in cell fate specification: a view from the nervous system. Cell *96*, 211–224.

Errington, J. (2003). Regulation of endospore formation in Bacillus subtilis. Nat. Rev. Microbiol. *1*, 117–126.

Gerke, J.P., Chen, C.T., and Cohen, B.A. (2006). Natural isolates of Saccharomyces cerevisiae display complex genetic variation in sporulation efficiency. Genetics *174*, 985–997.

Gilbert, S.F. (2006). Developmental Biology, Eighth Edition (Sunderland, MA: Sinauer Associates).

Gimeno, C.J., Ljungdahl, P.O., Styles, C.A., and Fink, G.R. (1992). Unipolar cell divisions in the yeast S. cerevisiae lead to filamentous growth: regulation by starvation and RAS. Cell *68*, 1077–1090.

Goldstein, J.C., Waterhouse, N.J., Juin, P., Evan, G.I., and Green, D.R. (2000). The coordinate release of cytochrome c during apoptosis is rapid, complete and kinetically invariant. Nat. Cell Biol. *2*, 156–162.

Gonzalez-Pastor, J.E., Hobbs, E.C., and Losick, R. (2003). Cannibalism by sporulating bacteria. Science *301*, 510–513.

Granot, D., Margolskee, J.P., and Simchen, G. (1989). A long region upstream of the IME1 gene regulates meiosis in yeast. Mol. Gen. Genet. *218*, 308–314.

Green, D.R. (2005). Apoptotic pathways: ten minutes to dead. Cell *121*, 671–674.

Griffioen, G., Anghileri, P., Imre, E., Baroni, M.D., and Ruis, H. (2000). Nutritional control of nucleocytoplasmic localization of cAMP-dependent protein kinase catalytic and regulatory subunits in Saccharomyces cerevisiae. J. Biol. Chem. *275*, 1449–1456.

Guttmann-Raviv, N., Martin, S., and Kassir, Y. (2002). Ime2, a meiosis-specific kinase in yeast, is required for destabilization of its transcriptional activator, Ime1. Mol. Cell. Biol. *22*, 2047–2056.

Halme, A., Bumgarner, S., Styles, C., and Fink, G.R. (2004). Genetic and epigenetic regulation of the FLO gene family generates cell-surface variation in yeast. Cell *116*, 405–415.

Harbison, C.T., Gordon, D.B., Lee, T.I., Rinaldi, N.J., Macisaac, K.D., Danford, T.W., Hannett, N.M., Tagne, J.B., Reynolds, D.B., Yoo, J., et al. (2004). Transcriptional regulatory code of a eukaryotic genome. Nature *431*, 99–104.

Honigberg, S.M., and Purnapatre, K. (2003). Signal pathway integration in the switch from the mitotic cell cycle to meiosis in yeast. J. Cell Sci. *116*, 2137–2147.

Horesh, O., Simchen, G., and Friedmann, A. (1979). Morphogenesis of the synapton during yeast meiosis. Chromosoma *75*, 101–115.

Kane, S.M., and Roth, R. (1974). Carbohydrate metabolism during ascospore development in yeast. J. Bacteriol. *118*, 8–14.

Kassir, Y., Granot, D., and Simchen, G. (1988). IME1, a positive regulator gene of meiosis in S. cerevisiae. Cell *52*, 853–862.

Kussell, E., and Leibler, S. (2005). Phenotypic diversity, population growth, and information in fluctuating environments. Science *309*, 2075–2078.

Mandel, S., Robzyk, K., and Kassir, Y. (1994). IME1 gene encodes a transcription factor which is required to induce meiosis in Saccharomyces cerevisiae. Dev. Genet. *15*, 139–147.

Nagai, T., Ibata, K., Park, E.S., Kubota, M., Mikoshiba, K., and Miyawaki, A. (2002). A variant of yellow fluorescent protein with fast and efficient maturation for cell-biological applications. Nat. Biotechnol. *20*, 87–90.

Padmore, R., Cao, L., and Kleckner, N. (1991). Temporal comparison of recombination and synaptonemal complex formation during meiosis in S. cerevisiae. Cell *66*, 1239–1256.

Pedraza, J.M., and Paulsson, J. (2007). Random timing in signaling cascades. Mol. Syst. Biol. *3*, 81. Published online February 13, 2007. 10.1038/msb4100121.

Pnueli, L., Edry, I., Cohen, M., and Kassir, Y. (2004). Glucose and nitrogen regulate the switch from histone deacetylation to acetylation for expression of early meiosis-specific genes in budding yeast. Mol. Cell. Biol. *24*, 5197–5208.

Primig, M., Williams, R.M., Winzeler, E.A., Tevzadze, G.G., Conway, A.R., Hwang, S.Y., Davis, R.W., and Esposito, R.E. (2000). The core meiotic transcriptome in budding yeasts. Nat. Genet. *26*, 415–423.

Rubin-Bejerano, I., Mandel, S., Robzyk, K., and Kassir, Y. (1996). Induction of meiosis in Saccharomyces cerevisiae depends on conversion of the transcriptional represssor Ume6 to a positive regulator by its regulated association with the transcriptional activator Ime1. Mol. Cell. Biol. *16*, 2518–2526.

Rubin-Bejerano, I., Sagee, S., Friedman, O., Pnueli, L., and Kassir, Y. (2004). The in vivo activity of Ime1, the key transcriptional activator of meiosis-specific genes in Saccharomyces cerevisiae, is inhibited by the cyclic AMP/protein kinase A signal pathway through the glycogen synthase kinase 3-beta homolog Rim11. Mol. Cell. Biol. *24*, 6967–6979.

Sagee, S., Sherman, A., Shenhar, G., Robzyk, K., Ben-Doy, N., Simchen, G., and Kassir, Y. (1998). Multiple and distinct activation and repression sequences mediate the regulated transcription of IME1, a transcriptional activator of meiosis-specific genes in Saccharomyces cerevisiae. Mol. Cell. Biol. *18*, 1985–1995.

Shefer-Vaida, M., Sherman, A., Ashkenazi, T., Robzyk, K., and Kassir, Y. (1995). Positive and negative feedback loops affect the transcription of IME1, a positive regulator of meiosis in Saccharomyces cerevisiae. Dev. Genet. *16*, 219–228.

Shenhar, G., and Kassir, Y. (2001). A positive regulator of mitosis, Sok2, functions as a negative regulator of meiosis in Saccharomyces cerevisiae. Mol. Cell. Biol. *21*, 1603–1612.

Sherman, A., Shefer, M., Sagee, S., and Kassir, Y. (1993). Post-transcriptional regulation of IME1 determines initiation of meiosis in Saccharomyces cerevisiae. Mol. Gen. Genet. *237*, 375–384.

Simchen, G., and Kassir, Y. (1989). Genetic regulation of differentiation towards meiosis in the yeast Saccharomyces cerevisiae. Genome *31*, 95–99.

Simchen, G., Pinon, R., and Salts, Y. (1972). Sporulation in Saccharomyces cerevisiae: premeiotic DNA synthesis, readiness and commitment. Exp. Cell Res. *75*, 207–218.

Thattai, M., and van Oudenaarden, A. (2004). Stochastic gene expression in fluctuating environments. Genetics *167*, 523–530.

Vidan, S., and Mitchell, A.P. (1997). Stimulation of yeast meiotic gene expression by the glucose-repressible protein kinase Rim15p. Mol. Cell. Biol. *17*, 2688–2697.

Wang, Y., Liu, C.L., Storey, J.D., Tibshirani, R.J., Herschlag, D., and Brown, P.O. (2002). Precision and functional specificity in mRNA decay. Proc. Natl. Acad. Sci. USA *99*, 5860–5865.

Williams, R.M., Primig, M., Washburn, B.K., Winzeler, E.A., Bellis, M., Sarrauste de Menthiere, C., Davis, R.W., and Esposito, R.E. (2002). The Ume6 regulon coordinates metabolic and meiotic gene expression in yeast. Proc. Natl. Acad. Sci. USA *99*, 13431–13436.

Williamson, D.H., Johnston, L.H., Fennell, D.J., and Simchen, G. (1983). The timing of the S phase and other nuclear events in yeast meiosis. Exp. Cell Res. *145*, 209–217.

Wolf, D.M., Vazirani, V.V., and Arkin, A.P. (2005). Diversity in times of adversity: probabilistic strategies in microbial survival games. J. Theor. Biol. *234*, 227–253.

Xiao, Y., and Mitchell, A.P. (2000). Shared roles of yeast glycogen synthase kinase 3 family members in nitrogen-responsive phosphorylation of meiotic regulator Ume6p. Mol. Cell. Biol. *20*, 5447–5453.